Received: 13 April 2018 | Revised: 29 June 2018 | Accepted: 7 August 2018

DOI: 10.1002/met.1755

Meteorological Applications RMetS

RESEARCH ARTICLE

# Customization of the Advanced Research Weather Research and Forecasting model over the Singapore region: impact of planetary boundary layer schemes, land use, land cover and model horizontal grid resolution

Srikanth Madala[1] | Santo V. Salinas[1] | Jun Wang[2,3] | Soo Chin Liew[1]

[1]Centre for Remote Imaging Sensing and Processing, National University of Singapore, Singapore

[2]Center for Global and Regional Environmental Research, University of Iowa, Iowa City, Iowa

[3]Department of Chemical and Biochemical Engineering, University of Iowa, Iowa City, Iowa

**Correspondence**
Srikanth Madala, Research Scientist, Centre for Remote Imaging, Sensing and Processing (CRISP), National University of Singapore (NUS), Singapore-119076, Singapore.
Email: srikanthaesi@gmail.com

Accurate simulations of surface meteorological variables are important for the transport and dispersion of air pollutants and air quality in the lower atmosphere. In the present study, the surface meteorological variables over Singapore were simulated using the Advanced Research Weather Research and Forecasting (WRF-ARW) mesoscale model. The sensitivity tests were conducted with six different planetary boundary layer (PBL) schemes (Yonsei University, Mellor–Yamada–Janjic, University of Washington, Asymmetric Convective Model version 2 [ACM2], Bougeault–Lacarrère, Quasi-Normal Scale Elimination), four different horizontal grid resolutions (27, 9, 3 and 1 km) and two different land use, land cover datasets (US Geological Survey [USGS] and Moderate Resolution Imaging Spectroradiometer [MODIS]). Eight days (January 20–28, 2015) were selected for the WRF-ARW model simulations for simulating surface meteorological variables. The model results were validated with available observations over the Singapore region. A lower mean bias, mean absolute error and root mean square error and good correlation were found in calculating surface meteorological variables with increase in the WRF-ARW model horizontal resolution up to 3 km. Further, MODIS land use, land cover datasets considerably improved the prediction of surface meteorological variables compared to the USGS for all PBL schemes and horizontal grid resolutions. Qualitative and quantitative analyses of the surface meteorological variables simulated using the ACM2 PBL scheme with 3 km horizontal grid resolution with MODIS land use, land cover data are in better agreement with observations with less error and a good correlation coefficient. The better performance by ACM2 could be due to non-local turbulence closure during unstable conditions and local closure during the stable and neutral conditions formulated in this scheme. Overall, this study indicates possibilities to improve regional level air quality monitoring and prediction capabilities over Singapore.

KEYWORDS

planetary boundary layer, USGS and MODIS, WRF-ARW model

## 1 | INTRODUCTION

Over the last few decades, fast industrialization and urbanization in southeast Asia has led to a considerable degradation of land use and substantial deterioration of regional air quality. Regional modelling of air quality indicators needs a correct representation of meteorological variables so that realistic estimation of pollutant concentrations can be obtained. Atmospheric models are very useful for predicting short range weather and many issues need to be considered to simulate small scale and mesoscale circulations (Hanna and Yang, 2001). Planetary boundary layer (PBL) processes are very important for the evolution of low level flow-field variables, surface meteorological variables and other parameters that affect the transport and dispersion of air pollutants. The assessment of air pollution by using atmospheric models deals with a number of problems such as the impact of horizontal and vertical resolutions, initialization and PBL schemes (Baker *et al*., 2013). Horizontal and vertical resolutions are one of the important issues in mesoscale atmospheric models (Gego *et al*., 2005; Chou, 2011).

*In situ* observations of meteorological variables are limited in most regions of the world, but air quality models need gridded meteorological data. Hence, meteorological models can be used to generate gridded meteorological variables for air quality modelling. Thus, the uncertainties of the meteorological model have a negative influence on air quality model results (Sistla *et al*., 1996; Kumar *et al*., 2017). There is no unique set of physics parameterization options that can simulate all the meteorological variables accurately at all model grid points. The performance of the Advanced Research Weather Research and Forecasting (WRF-ARW) model depends on model resolution (horizontal and vertical), land use, land cover, PBL parameterization schemes (Madala *et al*., 2014; Shrivastava *et al*., 2015).

In general, an increase in the horizontal grid resolution of atmospheric models increases the ability to resolve the topographical features and land use, land cover characteristics. It is difficult to define the horizontal grid spacing in order to achieve a preferred level of accuracy. The model sensitivity to horizontal resolution has been calculated to define optimum grid spacing for better simulation of meteorological variables over a particular region. Fita *et al*. (2010) studied the WRF-ARW model sensitivity to horizontal and vertical resolution and concluded that simulations with high resolution give better representation of the atmospheric features, especially over complex terrain. A study by Giannakopoulou and Nhili (2014) on the sensitivity of the WRF-ARW model with different horizontal grid resolutions, initial and boundary conditions, PBL parameterization schemes and increased nested domains reveals that the simulation with 3 km horizontal grid resolution gives better results than 1 km grid spacing. Tan *et al*. (2013) evaluated the performance of the WRF-ARW model for a short-term wind energy prediction system for Turkey. In that work, it was noticed that a coarser resolution (3 km) simulated extreme wind cases better than a fine resolution (1 km).

Numerous studies have highlighted the role of PBL schemes in the simulation of atmospheric circulations by using atmospheric mesoscale models (e.g. Hu *et al*., 2010; Shin and Hong, 2011; Floors *et al*., 2013; Yang *et al*., 2013). Several recent studies over the tropical Indian region emphasize the role of PBL schemes in atmospheric simulations by using mesoscale models for accurate representation of surface meteorological variables as well as the thermodynamic vertical structure of the atmosphere (Hariprasad *et al*., 2014; Madala *et al*., 2015, 2017; Rahul *et al*., 2016; Preeti and Manju, 2017). Over the Singapore region, there are relatively limited studies on the performance of atmospheric models (e.g. Li *et al*., 2013, 2016; Singh *et al*., 2015) in the context of surface meteorological variables. Li *et al*. (2013) employed WRF with a single-layer urban canopy model to examine the urban atmosphere of the Singapore region. The results showed that anthropogenic heat played an important role in surface fluxes, temperature, relative humidity (RH) and PBL height. Singh *et al*. (2015) predicted the monsoon and inter-monsoon periods over Singapore by using the WRF-ARW model with high-resolution land use and sea surface temperature datasets. That study highlights that model accuracy is improved by approximately 10% with high-resolution datasets. Li *et al*. (2016) studied the influence of urbanization patterns over the local weather of the Singapore region. They found that rainfall is more strongly influenced by sea breezes than the urbanization pattern over Singapore. From the literature review, it is noticed that studies on PBL schemes using atmospheric modelling for surface meteorological variables are very limited over the Singapore region. In the present study, an attempt was made to examine the surface meteorological variables over the Singapore region by using the WRF-ARW mesoscale model. The aim of the study was to evaluate the performance of the WRF-ARW model to simulate surface meteorological variables by conducting sensitivity experiments with six different PBL schemes, four different horizontal grid resolutions and two different land use, land cover datasets.

## 2 | STUDY REGION

The study region for the present investigation was Singapore (1 ° 17 ′ 24.97 ″ N, 103 ° 51 ′ 7.05 ″ E), an island city-state

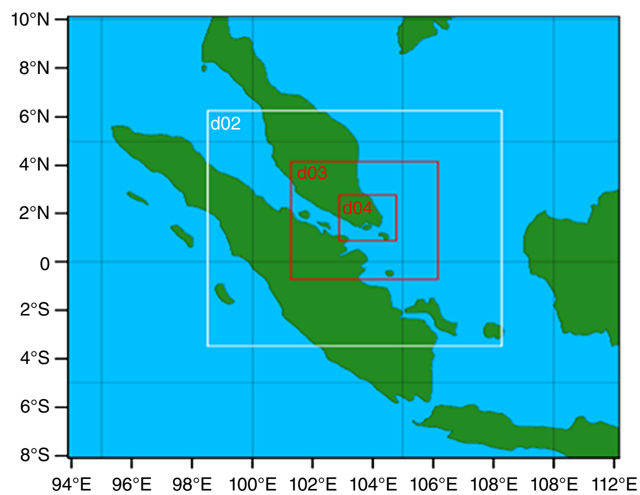


**FIGURE 1** Nested domains used in the Advanced Research Weather Research and Forecasting model [Colour figure can be viewed at wileyonlinelibrary.com]

**TABLE 1** Overview of the Advanced Research Weather Research and Forecasting model configuration over Singapore

| Dynamics | Non-hydrostatic |
|---|---|
| Initial and boundary data | NCEP FNL |
| Temporal interval of boundary data | 6 hr |
| Grid size | Domain 1: (76 × 76) × 51<br>Domain 2: (121 × 121) × 51<br>Domain 3: (181 × 181) × 51<br>Domain 4: (211 × 211) × 51 |
| Resolution | Domain 1: 27 × 27 km<br>Domain 2: 9 × 9 km<br>Domain 3: 3 × 3 km<br>Domain 4: 1 × 1 km |
| Map projection | Mercator |
| Horizontal grid system | Arakawa-C grid |
| Integration time step for outermost domain | 90 s |
| Vertical coordinates | 51 vertical levels |
| Time integration scheme | Third order Runga–Kutta scheme |
| Spatial differencing scheme | Sixth order centre differencing |
| PBL schemes | YSU, MYJ, QNSE, MYNN2, ACM2 and UM |
| Cumulus parameterization | Kain–Fritsch scheme |
| Surface layer parameterization | Noah land surface scheme |
| Microphysics | Goddard microphysics scheme |
| Short wave radiation | Dudhia scheme |
| Long wave radiation | RRTM scheme |
| Terrain and land use data | USGS and MODIS |

*Note.* MYNN2: Mellor–Yamada–Nakanishi–Niino Level 2.

off southern Malaysia with a surface area of 700 km$^2$ and a population of 6 million. It has an average elevation of 15 m above sea level.

## 3 | DATA AND METHODOLOGY

### 3.1 | Data

Surface meteorological observations from Weather Underground (Changi 1.366 ° N, 103.983 ° E; Seleta 1.4166 ° N, 103.86 ° E; Paya Lebar 1.36 ° N, 103.90 ° E) (http://www.wunderground.com/history) and from the National University of Singapore (NUS) (1.296 ° N, 103.776 ° E) (http://www.fas.nus.edu.sg/geog/weather/) at every 1 hr interval are used for model validation. To study the influence of land use and land cover on the model simulated surface layer parameters, two land cover datasets (the US Geological Survey [USGS] and the Moderate Resolution Imaging Spectroradiometer [MODIS]) were used. The model was initialized with final analysis (FNL) data with a resolution of 1° × 1°.

### 3.2 | Mesoscale model

The WRF-ARW mesoscale model version 3.8 was used for the present study. The horizontal and vertical resolutions play a critical role in the simulation of small scale atmospheric features. For this purpose, the WRF-ARW mesoscale model had four nested domains having horizontal grid resolutions of 27, 9, 3 and 1 km and 51 unequally spaced vertical sigma-pressure levels with the top of the model at 50 hPa (Figure 1). The spatial figure for both MODIS and USGS for all domains (Figures S1 and S2). The model was initialized at 1200 UTC and integrated 60 hr for all simulations. In each simulation, the first 12 hr was considered as the model spin-up. The model simulations started at 1200 UTC on January 19, 21, 23 and 25, 2015; the WRF-ARW model configuration for the present study is presented in Table 1. The

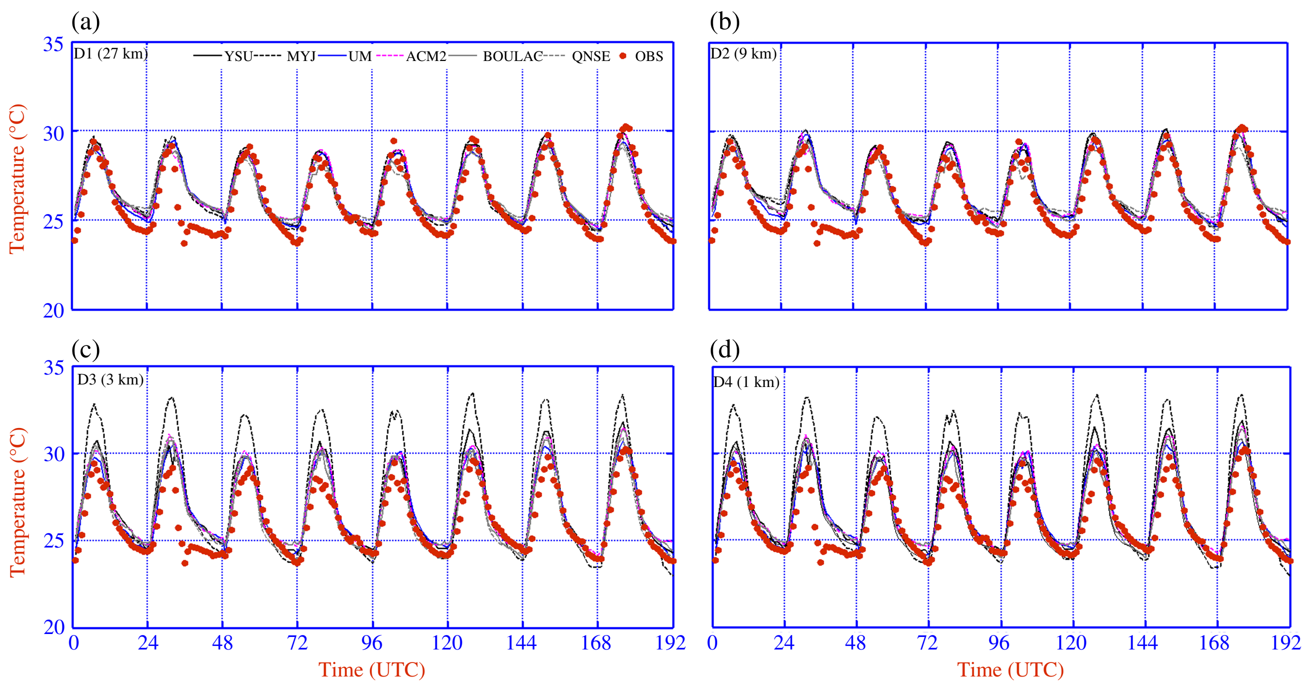


**FIGURE 2** Comparison of Advanced Research Weather Research and Forecasting model simulations of air temperature at 2 m with the US Geological Survey at different horizontal resolutions over the National University of Singapore during January 20–28, 2015 with available observations [Colour figure can be viewed at wileyonlinelibrary.com]

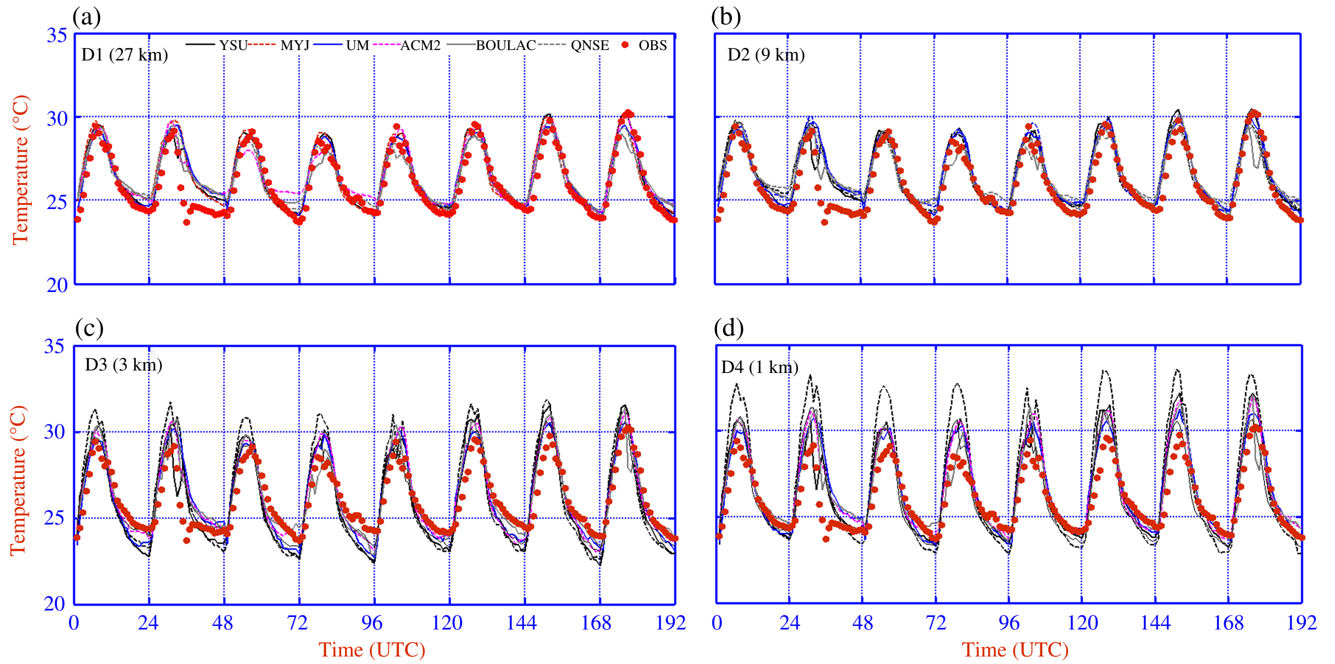


**FIGURE 3** Comparison of Advanced Research Weather Research and Forecasting model simulations of air temperature at 2 m with the Moderate Resolution Imaging Spectroradiometer at different horizontal resolutions over the National University of Singapore during January 20–28, 2015 with available observations [Colour figure can be viewed at wileyonlinelibrary.com]

WRF-ARW model was initialized with 6 hr National Centers for Environmental Prediction (NCEP) FNL data with 1.0°× 1.0° for the initial and boundary conditions. The sensitivity tests were conducted with various PBL schemes, namely two non-local (Yonsei University [YSU] and Asymmetric Convective Model version 2 [ACM2]) and four local turbulent kinetic energy closures (Mellor–Yamada–Janjic [MYJ], Quasi-Normal Scale Elimination [QNSE], Bougeault–Lacarrère [BOULAC] and University of Washington [UM]). Shin and Hong (2011), Hariprasad *et al.* (2014) and Kleczek *et al.* (2014) give details of the PBL parameterization schemes. The model physics options used are the Kain–Fritsch scheme (Kain, 2004) for convective parameterization (not used for domains d03 and d04), the

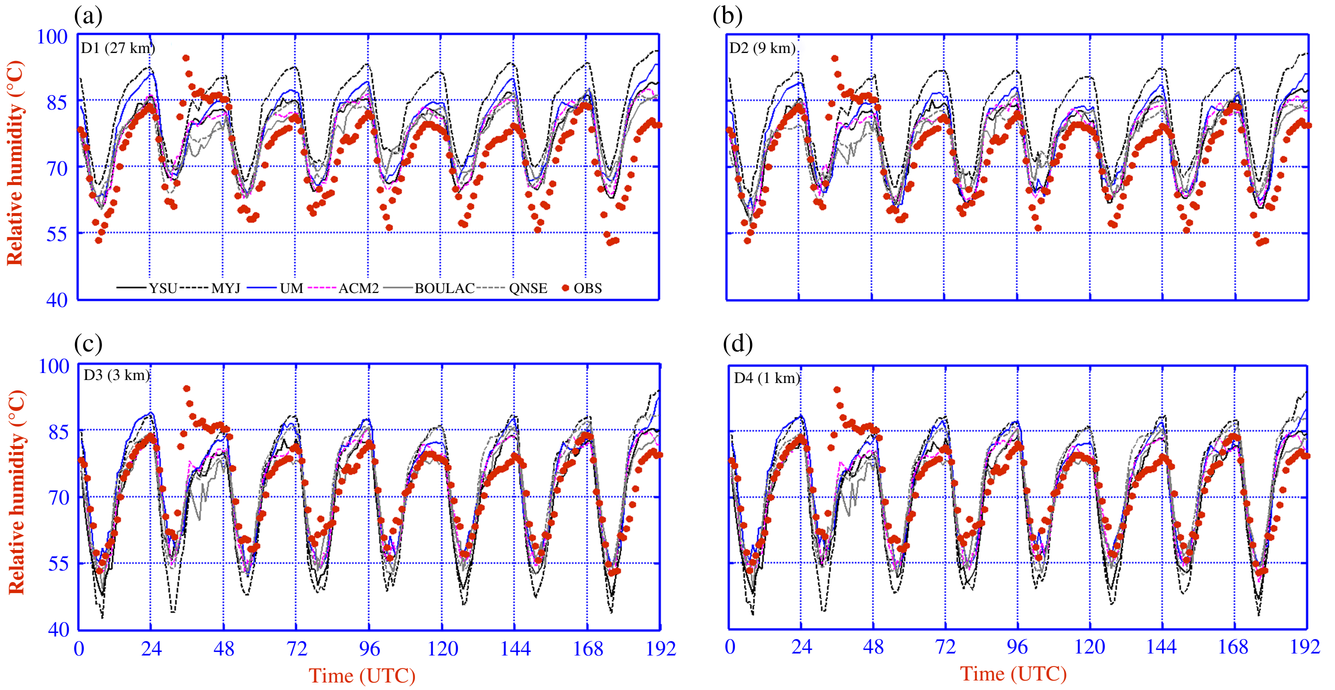


**FIGURE 4** Comparison of Advanced Research Weather Research and Forecasting model simulations of relative humidity with the US Geological Survey at different horizontal resolutions over the National University of Singapore during January 20–28, 2015 with available observations [Colour figure can be viewed at wileyonlinelibrary.com]

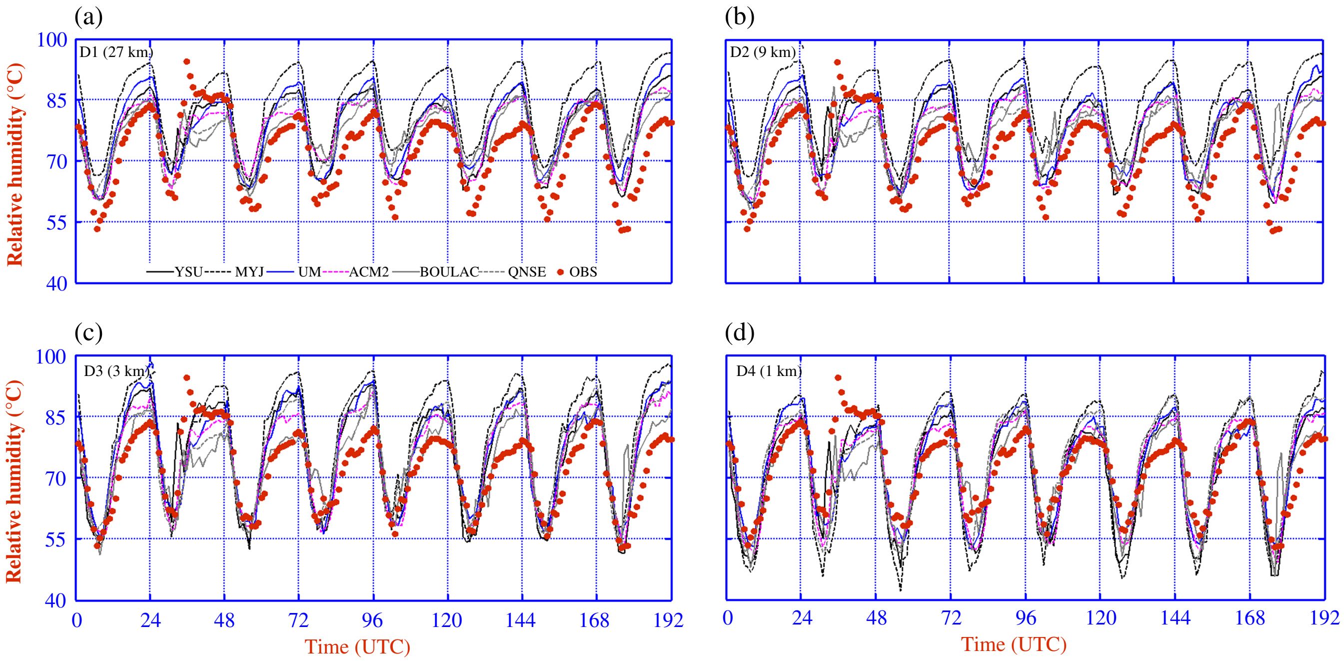


**FIGURE 5** Comparison of Advanced Research Weather Research and Forecasting model simulations of relative humidity with the Moderate Resolution Imaging Spectroradiometer at different horizontal resolutions over the National University of Singapore during January 20–28, 2015 with available observations [Colour figure can be viewed at wileyonlinelibrary.com]

Goddard microphysics scheme (Tao *et al.,* 2003; Singh *et al.*, 2017) for cloud microphysics, the Noah land surface model (Chen and Dudia, 2001) for surface physics, the Rapid Radiative Transfer Model (Mlawer *et al.,* 1997) for long wave radiation processes and the Dudhia scheme for short wave radiation (Dudhia, 1989). All the physics options (except the PBL schemes) were taken from Singh *et al.* (2015). A detailed explanation of the model physics, equations and dynamics is presented in Skamarock *et al.* (2008).

## 4 | RESULTS AND DISCUSSION

### 4.1 | Variation in surface meteorological variables

Inter-comparison of the performance of six different PBL schemes (YSU, MYJ, UM, ACM2, BOULAC, QNSE), four different horizontal grid resolutions (27, 9, 3 and 1 km) and two different land use, land cover datasets (USGS and MODIS) from a WRF-ARW mesoscale model with

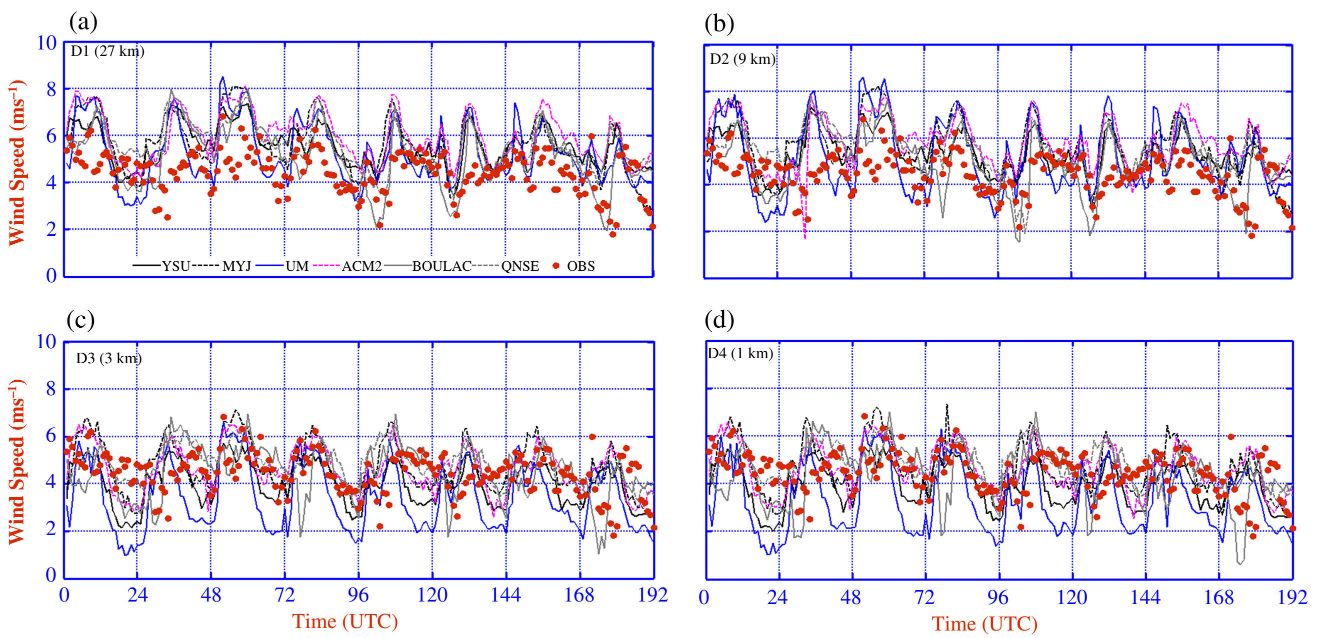


**FIGURE 6** Comparison of Advanced Research Weather Research and Forecasting model simulations of wind speed with the US Geological Survey at different horizontal resolutions over the National University of Singapore during January 20–28, 2015 with available observations [Colour figure can be viewed at wileyonlinelibrary.com]

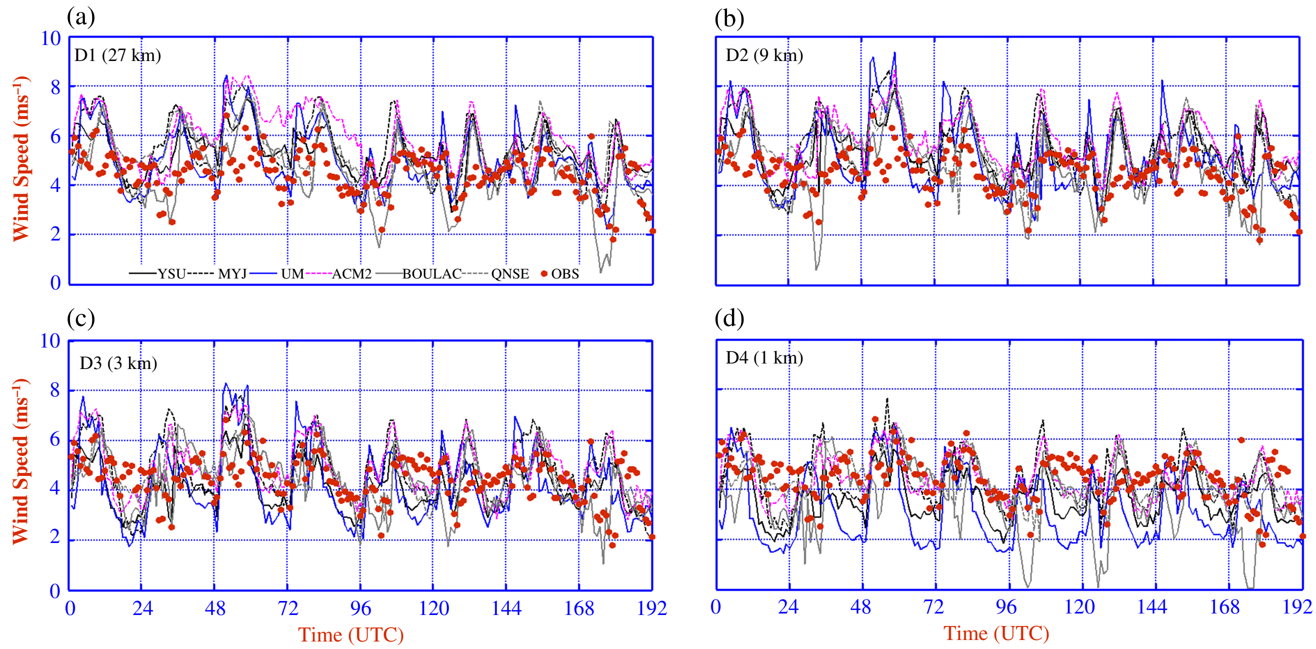


**FIGURE 7** Comparison of Advanced Research Weather Research and Forecasting model simulations of wind speed with the Moderate Resolution Imaging Spectroradiometer at different horizontal resolutions over the National University of Singapore during January 20–28, 2015 with available observations [Colour figure can be viewed at wileyonlinelibrary.com]

available observations is discussed in this section. The WRF-ARW model simulations of the diurnal variation of surface air temperature (AT) (°C) at 2 m, surface RH (%) at 2 m, surface wind speed (WS) (m/s) at 10 m and wind direction (WD) (degree) at 10 m along with available *in situ* hourly observations at the NUS are shown in Figures 2–9.

#### 4.1.1 | Diurnal variation of air temperature

The diurnal variation of AT simulated by various PBL parameterization schemes with different horizontal resolutions over 8 days (January 20–28, 2015) together with the available observations at the NUS station are depicted in Figure 2a–d for the USGS dataset and in Figure 3a–d for the

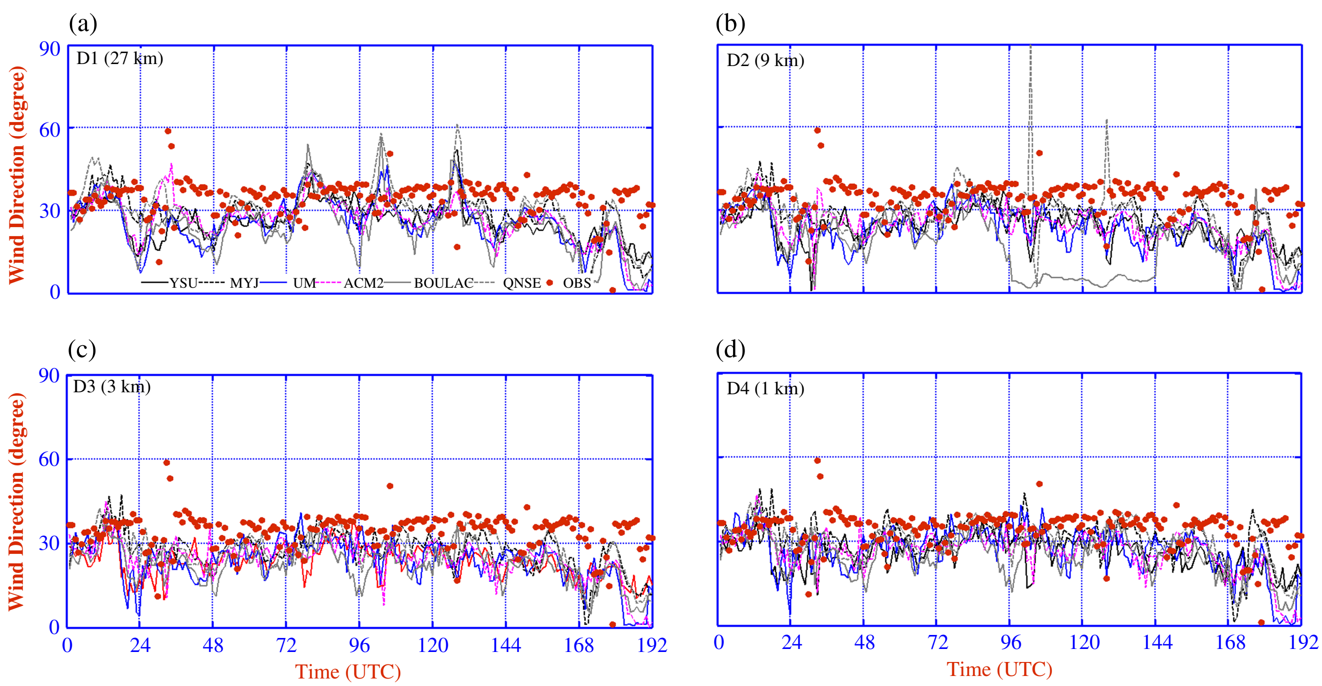


**FIGURE 8** Comparison of Advanced Research Weather Research and Forecasting model simulations of wind direction with the US Geological Survey at different horizontal resolutions over the National University of Singapore during January 20–28, 2015 with available observations [Colour figure can be viewed at wileyonlinelibrary.com]

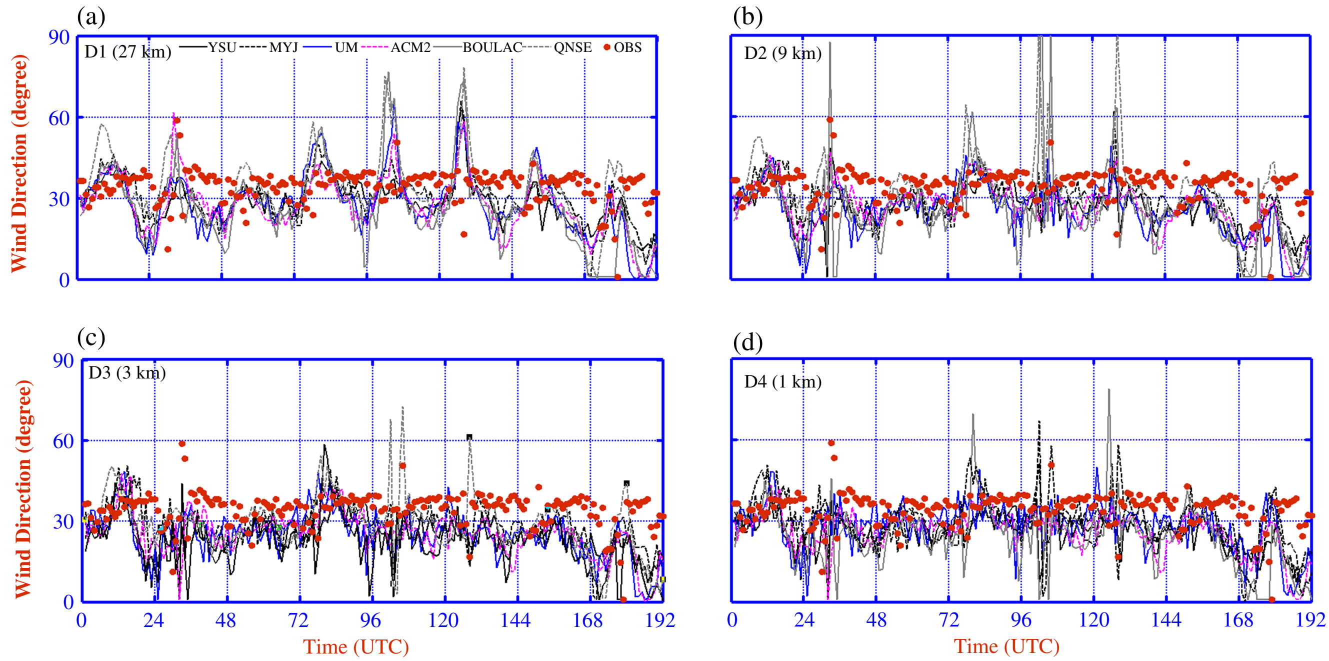


**FIGURE 9** Comparison of Advanced Research Weather Research and Forecasting model simulations of wind direction with the Moderate Resolution Imaging Spectroradiometer at different horizontal resolutions over the National University of Singapore during January 20–28, 2015 with available observations [Colour figure can be viewed at wileyonlinelibrary.com]

MODIS dataset respectively. It is noted that all PBL schemes simulate the diurnal variation of AT (daytime) reasonably well and a slight warm mean bias (model observation >0) (night time) for 27 and 9 km for both the USGS and the MODIS (Figure 2a,b). In the case of 3 and 1 km resolutions, all PBL schemes except the MYJ and

**TABLE 2** Percentage change of errors with the US Geological Survey (USGS) for different horizontal grid resolutions

| % change | Parameter | Errors | YSU | MYJ | UM | ACM2 | BOULAC | QNSE |
|---|---|---|---|---|---|---|---|---|
| USGS ([D2 – D1]/D1) × 100 | Air temperature | MAE | −15.5 | −8.9 | −11.5 | −12.0 | −15.0 | −12.9 |
| | | RMSE | −16.5 | −13.0 | −13.9 | −13.8 | −14.6 | −11.9 |
| | Relative humidity | MAE | −16.0 | −13.0 | −12.1 | −15.2 | −16.8 | −15.2 |
| | | RMSE | −13.7 | −11.1 | −11.4 | −12.6 | −14.4 | −13.0 |
| | Wind speed | MAE | −13.3 | −11.6 | −11.0 | −15.3 | −2.6 | −9.8 |
| | | RMSE | −9.4 | −9.1 | −8.2 | −12.4 | −2.6 | −8.5 |
| | Wind direction | MAE | 8.7 | 5.0 | 2.4 | 4.5 | 33.0 | 5.7 |
| | | RMSE | 4.8 | 2.7 | −20.8 | −13.0 | 22.9 | 24.2 |
| USGS ([D3 – D2]/D2) × 100 | Air temperature | MAE | −9.2 | 17.6 | −5.4 | −5.7 | 0.0 | −4.0 |
| | | RMSE | −5.4 | 22.0 | −5.9 | −3.6 | −1.8 | −3.2 |
| | Relative humidity | MAE | −2.9 | −14.5 | −8.3 | −7.1 | −11.3 | 3.3 |
| | | RMSE | 0.3 | −11.7 | −5.4 | −5.1 | −6.4 | 1.5 |
| | Wind speed | MAE | −18.7 | −19.0 | −7.5 | −23.8 | −0.7 | −16.2 |
| | | RMSE | −21.2 | −15.9 | −7.3 | −22.6 | −1.1 | −15.9 |
| | Wind direction | MAE | −0.8 | −1.6 | 1.6 | −1.4 | −23.1 | −6.6 |
| | | RMSE | −0.6 | −0.8 | 15.6 | −0.6 | −17.2 | −18.6 |
| USGS ([D4 –D3]/D3) × 100 | Air temperature | MAE | 5.1 | 11.7 | 4.6 | 3.6 | 4.7 | 10.3 |
| | | RMSE | 4.8 | 10.3 | 5.4 | 2.8 | 5.5 | 7.4 |
| | Relative humidity | MAE | 13.3 | 11.1 | 7.6 | 9.2 | 11.3 | 13.7 |
| | | RMSE | 12.4 | 16.7 | 9.4 | 9.3 | 11.1 | 10.9 |
| | Wind speed | MAE | 7.4 | 5.4 | 8.9 | 4.6 | 4.7 | 6.5 |
| | | RMSE | 6.6 | 4.2 | 7.8 | 3.7 | 6.0 | 7.2 |
| | Wind direction | MAE | 0.0 | 1.7 | −3.6 | −1.5 | −0.9 | 1.8 |
| | | RMSE | 1.0 | 2.3 | −13.4 | −0.3 | −0.1 | 0.4 |

*Note.* ACM2: Asymmetric Convective Model version 2; BOULAC: Bougeault–Lacarrère; MAE: mean absolute error; MYJ: Mellor–Yamada–Janjic; QNSE: Quasi-Normal Scale Elimination; RMSE: root mean square error; UM: University of Washington; YSU: Yonsei University.

**TABLE 3** Percentage change of errors with the Moderate Resolution Imaging Spectroradiometer (MODIS) for different horizontal grid resolutions

| % change | Parameter | Errors | YSU | MYJ | UM | ACM2 | BOULAC | QNSE |
|---|---|---|---|---|---|---|---|---|
| MODIS ([D2 – D1]/D1) × 100 | Air temperature | MAE | −14.7 | −10.3 | −13.0 | −18.7 | −16.1 | −12.1 |
| | | RMSE | −16.4 | −12.7 | −15.9 | −17.6 | −15.4 | −13.9 |
| | Relative humidity | MAE | −12.4 | −14.0 | −14.2 | −16.6 | −17.4 | −14.4 |
| | | RMSE | −9.5 | −10.6 | −11.7 | −13.9 | −12.2 | −12.0 |
| | Wind speed | MAE | −10.6 | −13.6 | −9.1 | −16.1 | −3.6 | −8.6 |
| | | RMSE | −11.2 | −11.2 | −8.2 | −13.9 | −3.4 | −7.6 |
| | Wind direction | MAE | 3.4 | 1.5 | 3.1 | 1.7 | 6.2 | −2.4 |
| | | RMSE | −10.3 | −12.7 | −8.7 | −10.4 | 3.3 | −12.2 |
| MODIS ([D3 – D2]/D2) × 100 | Air temperature | MAE | 21.0 | 40.6 | 12.5 | 4.1 | −5.1 | 9.6 |
| | | RMSE | 13.1 | 27.4 | 5.7 | 1.0 | −4.8 | 5.9 |
| | Relative humidity | MAE | 1.5 | −25.4 | −9.5 | −4.4 | −12.6 | 9.0 |
| | | RMSE | 3.4 | −18.6 | −3.3 | 0.4 | −10.2 | 7.2 |
| | Wind speed | MAE | −31.3 | −14.0 | −14.6 | −28.1 | −7.4 | −26.6 |
| | | RMSE | −28.6 | −11.3 | −11.5 | −27.8 | −6.5 | −24.1 |
| | Wind direction | MAE | 4.2 | 3.5 | 3.6 | 3.3 | −1.1 | 0.4 |
| | | RMSE | 16.5 | 18.0 | 15.0 | 12.3 | 0.8 | 18.4 |
| MODIS ([D3 – D3]/D3) × 100 | Air temperature | MAE | −9.2 | 5.9 | −4.4 | 0.0 | −1.4 | −4.9 |
| | | RMSE | −1.7 | 12.7 | 1.8 | 5.1 | 1.0 | −1.6 |
| | Relative humidity | MAE | 1.2 | −1.6 | −5.6 | 1.0 | 0.0 | 1.8 |
| | | RMSE | 0.3 | −2.9 | −5.3 | −1.1 | 1.9 | 0.6 |
| | Wind speed | MAE | 14.1 | 6.7 | 14.4 | −5.7 | 12.0 | 7.8 |
| | | RMSE | 12.8 | 5.2 | 13.7 | −4.6 | 10.1 | 7.0 |
| | Wind direction | MAE | 3.7 | 5.0 | −0.1 | 2.2 | 9.9 | −0.8 |
| | | RMSE | 12.1 | 2.7 | 0.2 | 1.9 | 24.1 | −2.4 |

*Note.* ACM2: Asymmetric Convective Model version 2; BOULAC: Bougeault–Lacarrère; MAE: mean absolute error; MYJ: Mellor–Yamada–Janjic; QNSE: Quasi-Normal Scale Elimination; RMSE: root mean square error; UM: University of Washington; YSU: Yonsei University.

YSU schemes closely simulated the AT during both daytime and night time. Compared to the USGS, the MODIS simulated AT well in comparison with the available observations (Figure 3a–d). It was found that, both in the MODIS and the USGS with coarse resolution (27 and 9 km), scheme to scheme variations in the simulated AT are very much less compared to fine resolution (3 and 1 km).

### 4.1.2 | Diurnal variation of relative humidity

The diurnal variations of RH with different land use, land cover datasets (USGS and MODIS) with different horizontal resolutions (27, 9, 3 and 1 km) over the study area, during January 20–28, 2015, together with observations are shown in Figures 4a–d and 5a–d respectively. It was found that the coarse resolution (i.e. 27 and 9 km) simulations overestimated RH during daytime and night time for all the PBL schemes for both the USGS and the MODIS (Figures 4a,b and 5a,b). The RH was better simulated during daytime except for the MYJ and YSU, whereas at night time RH was overestimated by all PBL schemes for both the USGS and the MODIS (Figures 4c,d and 5c,d). The RH was well simulated by the ACM2 followed by the BOULAC PBL scheme with realistic representation of diurnal variation.

### 4.1.3 | Diurnal variation of wind speed and wind direction

The comparison of simulated WS by using various PBL schemes and different horizontal resolutions over 8 days (January 20–28, 2015) with the available observations at the NUS is shown in Figures 6a–d and 7a–d (USGS and MODIS). It was found that WS was overestimated throughout the simulation time by both the USGS and the MODIS with 27 and 9 km grid resolutions. The coarse resolution simulations with the ACM2 and MYJ produced higher WS compared to other PBL parameterization schemes. Fine resolution simulations (3 and 1 km) are better simulated winds compared to the coarse resolutions (27 and 9 km) for both the USGS and MODIS (Figures 6 and 7). The fine resolution simulations with the UM and YSU followed by BOULAC produced weaker WS while the ACM2, MYJ and QNSE compared well with observations. The observed WD over the study region is mostly from the northnortheast and northeast during January 20–28, 2015 (Figures 8 and 9). All the PBL schemes simulated the WD well with both the USGS and MODIS land categories.

Moreover, the diurnal variation of these surface meteorological parameters compares well with the observations from the other three stations, Changi, Seleta and Paya Lebar. Based on qualitative comparisons, it is noticed that using the

**TABLE 4** Percentage change of errors with the US Geological Survey (USGS) and the Moderate Resolution Imaging Spectroradiometer (MODIS) (% change = {(MODIS – USGS)/MODIS} × 100)

| Domain (resolution) | Parameter | Errors | YSU | MYJ | UM | ACM2 | BOU LAC | QNSE |
|---|---|---|---|---|---|---|---|---|
| D1 (27 km) | Air temperature | MAE | −8.4 | −4.7 | −13.0 | −9.9 | −7.5 | −8.4 |
| | | RMSE | −3.9 | −2.8 | −8.7 | −9.2 | −5.7 | −4.4 |
| | Relative humidity | MAE | −3.6 | −7.6 | −8.5 | −9.1 | −8.7 | −3.6 |
| | | RMSE | −3.2 | −6.2 | −7.3 | −7.9 | −6.8 | −2.8 |
| | Wind speed | MAE | −7.5 | −10.7 | −14.7 | −16.7 | −10.7 | −7.9 |
| | | RMSE | −8.1 | −10.0 | −14.0 | −15.8 | −8.6 | −8.2 |
| | Wind direction | MAE | −4.8 | −2.8 | −10.0 | −7.0 | 0.9 | 6.1 |
| | | RMSE | −3.5 | −2.5 | −36.5 | −23.1 | 8.7 | 1.9 |
| D2 (9 km) | Air temperature | MAE | −7.4 | −6.3 | −15.0 | −18.9 | −9.0 | −7.4 |
| | | RMSE | −3.7 | −2.4 | −11.3 | −14.3 | −6.7 | −6.8 |
| | Relative humidity | MAE | 0.6 | −8.9 | −11.2 | −10.9 | −9.5 | −2.6 |
| | | RMSE | 1.6 | −5.6 | −7.7 | −9.5 | −4.2 | −1.6 |
| | Wind speed | MAE | −4.2 | −13.2 | −12.3 | −17.8 | −11.9 | −6.5 |
| | | RMSE | −10.3 | −12.6 | −14.0 | −17.8 | −9.5 | −7.1 |
| | Wind direction | MAE | −10.1 | −6.4 | −9.4 | −9.9 | −24.1 | −1.6 |
| | | RMSE | −20.8 | −20.6 | −18.4 | −19.4 | −8.6 | −38.8 |
| D3 (3 km) | Air temperature | MAE | 19.4 | 11.1 | 3.3 | −7.8 | −14.9 | 5.8 |
| | | RMSE | 13.2 | 1.9 | 0.9 | −9.1 | −10.1 | 2.4 |
| | Relative humidity | MAE | 4.9 | −24.8 | −12.7 | −7.7 | −11.1 | 2.7 |
| | | RMSE | 4.5 | −14.5 | −5.4 | −3.6 | −8.6 | 3.8 |
| | Wind speed | MAE | −23.2 | −6.7 | −21.6 | −24.8 | −20.0 | −21.6 |
| | | RMSE | −21.6 | −6.7 | −19.4 | −26.2 | −15.8 | −18.6 |
| | Wind direction | MAE | −4.8 | −1.2 | −7.2 | −5.0 | 3.5 | 5.5 |
| | | RMSE | −3.0 | −1.4 | −19.1 | −5.7 | 10.8 | 4.6 |
| D4 (1 km) | Air temperature | MAE | 6.7 | 6.3 | −5.8 | −11.7 | −21.9 | −9.2 |
| | | RMSE | 7.6 | 3.9 | −2.6 | −6.7 | −15.0 | −6.5 |
| | Relative humidity | MAE | −6.5 | −40.9 | −28.5 | −16.5 | −23.6 | −8.6 |
| | | RMSE | −7.0 | −37.6 | −21.8 | −14.5 | −18.4 | −6.1 |
| | Wind speed | MAE | −15.9 | −5.4 | −15.7 | −38.4 | −12.1 | −20.0 |
| | | RMSE | −14.9 | −5.7 | −13.3 | −37.1 | −11.5 | −18.8 |
| | Wind direction | MAE | −1.0 | 1.9 | −3.4 | −1.2 | 12.9 | 3.0 |
| | | RMSE | 7.2 | −1.1 | −2.9 | −3.4 | 28.2 | 1.8 |

*Note.* ACM2: Asymmetric Convective Model version 2; BOULAC: Bougeault–Lacarrère; MAE: mean absolute error; MYJ: Mellor–Yamada–Janjic; QNSE: Quasi-Normal Scale Elimination; RMSE: root mean square error; UM: University of Washington; YSU: Yonsei University.

ACM2 PBL scheme with MODIS land use data at 3 km grid resolution simulated surface meteorological variables realistically better than the other tested PBL parameterization schemes.

### 4.2 | Statistical analysis

A statistical analysis was done to quantify the model errors of the simulated variables. The error metrics (mean bias, mean absolute error, root mean square error and correlation coefficient) were calculated for the parameters AT and RH at 2 m and WS and WD at 10 m for four stations (total sample size $N = 703$) (Tables S1 and S2). The observed mean AT over the study period was 26.91 °C. It seems that all the PBL schemes captured a cold bias at all horizontal grid resolutions (27, 9, 3 and 1 km) for both the USGS and the MODIS. The ACM2, BOULAC and YSU PBL schemes generated smaller errors and higher correlation values than the other schemes. The observed mean RH during the study period was 73.36%. All PBL schemes generated a humidity bias for both the USGS and the MODIS at all horizontal grid resolutions. Relatively smaller errors and reasonable correlations were obtained for RH with the ACM2, YSU and BOULAC schemes, which indicated better performance than the other PBL schemes. The observed mean WS was 4.54 m/s. An overestimation of WS was found by all the PBL parameterization schemes with both the USGS and the MODIS for all horizontal grid resolutions. However, smaller errors and good correlations were found for the MYJ followed by the ACM2 and YSU, indicating that these PBL schemes simulate WS and WD relatively well. The percentage changes in errors for the aforementioned surface parameters with the

USGS and the MODIS with different horizontal grid resolutions and different PBL schemes are shown in Tables 2 and 3. It is clear that fine resolutions (i.e. 3 and 1 km) with the USGS and the MODIS generate less error and show high correlation compared to coarse resolutions (27 and 9 km). In addition, it was found that the errors are reduced from the mother domain to the nested domain (from d01 to d02 and d02 to d03). High-resolution (1 km) simulations will substantially increase the model numerical costs and time compared to the 3 km grid. Between d03 and d04 the results did not improve much with the USGS except for WD for some of the PBL schemes and mixed results were noticed for the MODIS. The error percentage change from the USGS and the MODIS is presented in Table 4. Overall, simulations with the MODIS generate lower errors for all surface meteorological variables compared to the simulations with the USGS at all horizontal resolutions. Based on the present analysis, it can be concluded that the MODIS at 3 km resolution with the ACM2 followed by the YSU and MYJ PBL schemes gives better representation of surface meteorological parameters compared to other schemes.

## 5 | SUMMARY AND CONCLUSIONS

The local surface meteorological variables play a significant role in air pollution transport and dispersion and air quality. The main goal of the present study was to assess the impact of six different planetary boundary layer (PBL) schemes, four different horizontal grid resolutions and two different land use, land cover datasets on the performance of the Advanced Research Weather Research and Forecasting (WRF-ARW) model for better simulation of the surface meteorological variables over the Singapore region. This study shows that the WRF-ARW model can capture the surface meteorological parameters reasonably well, validated with available observations over the study region. Statistical errors such as mean bias, mean absolute error, root mean square error and the correlation coefficient were evaluated and it was found that the Asymmetric Convective Model version 2 (ACM2) PBL scheme gives better simulation of various surface meteorological variables over the study region compared to the other PBL schemes. The improvement in the various meteorological variables with ACM2 could be due to the application of non-local diffusion during daytime under unstable conditions and local parameterization during stable night conditions. Further, Moderate Resolution Imaging Spectroradiometer (MODIS) land use, land cover data considerably improved the prediction of surface meteorological variables compared to the US Geological Survey for all PBL schemes and horizontal grid resolutions. For experiments using different horizontal resolutions, increasing the grid resolution from 27 to 9 km and from 9 to 3 km showed improvements (less error) but from 3 to 1 km did not show much improvement. It is concluded that 3 km horizontal grid resolution is the best resolution and that the finest 1 km spacing does not bring much improvement in the WRF-ARW model (Tan *et al*., 2013; Giannakopoulou and Nhili, 2014; Madala *et al*., 2014). This may be due to improper representation of land use, land cover data, which needs further investigation. However, this study is preliminary in nature and advocates the usefulness of the WRF-ARW model. Within its limitations, it is suggested that the WRF-ARW mesoscale model with the ACM2 PBL scheme with 3 km horizontal grid resolution and the MODIS land cover data is suitable over the Singapore region for better representation of surface meteorological parameter variables. This customization of the WRF-ARW model is found to be efficient but requires analysis of more days over the study region before any comprehensive conclusion can be reached.

## ACKNOWLEDGEMENT

Thanks are due to the Office for Space Technology and Industry Space Research Program (OSTIn, project number S15-1319-NRF OSTIn-SRP) for their generous funding for this study. Dr Srikanth Madala is grateful to the National University of Singapore (NUS) for providing the necessary facilities to conduct this research work. The authors are grateful to the anonymous reviewers for their useful suggestions in improving the quality of the paper.

## ORCID

*Srikanth Madala* https://orcid.org/0000-0003-2781-1586

## REFERENCES

Baker, K.R., Misenis, C., Obland, M.D., Scarino, R.A. and Kelly, J.T. (2013) Evaluation of surface and upper air fine scale WRF-ARW meteorological modeling of the May and June 2010 CalNex period in California. *Atmospheric Environment*, 80, 299–309.

Chen, F. and Dudhia, J. (2001) Coupling an advanced land-surface/ hydrology model with the Penn State/ NCAR MM5 modeling system. Part I: model description and implementation. *Monthly Weather Review*, 129, 569–585.

Chou, S.H. (2011) An example of vertical resolution impact on WRF-Var analysis. *Electronic Journal of Operational Meteorology*, 12, 1–20.

Dudhia, J. (1989) Numerical study of convection observed during the winter monsoon experiment using a mesoscale two-dimensional model. *Journal of the Atmospheric Sciences*, 46, 3077–3107.

Fita, L., Fernández, J., García-Díez, M. and Gutiérrez, J.M. (2010) SeaWind project: analysing the sensitivity on horizontal and vertical resolution on WRF simulations," in *Proceedings of the 2nd Meeting on Meteorology and Climatology of the Western Mediterranean* (JMCMO '10), 11-12 March 2010 in Valencia, Spain.

Floors, R., Vincent, C.L., Gryning, S.E., Pe, A. and Batchvarova, E. (2013) The wind profile in the coastal boundary layer: wind lidar measurements and numerical modelling. *Boundary-Layer Meteorology*, 147(3), 469–491.

Gego, E., Hogrefe, C., Kallos, G., Voudouri, A. and Irwin Rao, S. (2005) Examination of model predictions at different horizontal grid resolutions. *Environmental Fluid Mechanics*, 5, 63–85.

Giannakopoulou, E.M. and Nhili, R. (2014) WRF model methodology for offshore wind energy applications. *Advances in Meteorology*, 14, 319819. https://doi.org/10.1155/2014/319819.

Hanna, S. and Yang, R. (2001) Evaluations of mesoscale models' simulations of near-surface winds, temperature gradients, and mixing depths. *Journal of Applied Meteorology*, 40, 1095–1104.

Hariprasad, K.B.R.R., Srinivas, C.V., Bagavath Singh, A., Vijaya Bhaskara Rao, S., Baskaran, R. and Venkatraman, B. (2014) Numerical simulation and intercomparison of boundary layer structure with different PBL schemes in WRF using experimental observations at a tropical site. *Atmospheric Research*, 145, 27–44.

Hu, X.-M., Nielsen-Gammon, J. and Zhang, F. (2010) Evaluation of three planetary boundary layer schemes in the WRF model. *Journal of Applied Meteorology and Climatology*, 49, 1831–1844.

Kain, J.S. (2004) The Kain–Fritsch convective parameterization: an update. *Journal of Applied Meteorology*, 43(1), 170–181.

Kleczek, M.A., Steeneveld, G.J. and Holtslag, A.A.M. (2014) Evaluation of the weather research and forecasting mesoscale model for GABLS3: impact of boundary-layer schemes, boundary conditions and spin-up. *Boundary-Layer Meteorology*, 152(2), 213–243.

Kumar, A., Patil1, R.S., Dikshit, A.K. and Kumar, R. (2017) Application of WRF model for air quality modelling and AERMOD – a survey. *Aerosol and Air Quality Research*, 17, 1825–1837.

Li, X.-X., Koh, T.-Y., Entekhabi, D., Roth, M., Panda, J. and Norford, L.K. (2013) A multi-resolution ensemble 125 study of a tropical urban environment and its interactions with the background regional atmosphere. *Journal of Geophysical Research: Atmospheres*, 118, 9804–9818.

Li, X.-X., Koh, T.-Y., Panda, J. and Norford, L.K. (2016) Impact of urbanization patterns on the local climate of a tropical city, Singapore: an ensemble study. *Journal of Geophysical Research: Atmospheres*, 121, 4386–4403.

Madala, S., Satyanarayana, A.N. and Srinivas, C.V. (2017) Performance of WRF for simulation of mesoscale meteorological characteristics for air quality assessment over tropical Coastal City, Chennai. *Pure and Applied Geophysics*, 175, 501–518. https://doi.org/10.1007/s00024-017-1662-3.

Madala, S., Satyanarayana, A.N.V., Srinivas, C.V., Boadh, R. and Kumar, M. (2014) Performance evaluation of PBL schemes and horizontal resolution of WRF-ARW model over a hilly station. In: *Proceedings of ICTACEM 2014. International Conference on Theoretical, Applied, Computational and Experimental Mechanics (ICTACEM)*, 29–31 December 2014, IIT Kharagpur, India.

Madala, S., Satyanarayana, A.N.V., Srinivas, C.V. and Kumar, M. (2015) Mesoscale atmospheric flow-field simulations for air quality modelling over complex terrain region of Ranchi in eastern India using WRF. *Atmospheric Environment*, 107, 315–328.

Mlawer, E.J., Taubman, S.J., Brown, P.D., Iacono, M.J. and Clough, S.A. (1997) Radiative transfer for inhomogeneous atmosphere: RRTM, a validated correlated-k model for the longwave. *Journal of Geophysical Research*, 102(D14), 16663–16682.

Preeti, G. and Manju, M. (2017) Sensitivity of WRF model estimates to various PBL parameterizations in different climatic zones over India. *Atmospheric Research*, 194, 43–65.

Rahul, B., Satyanarayana, A.N.V., Rama Krishna, T.V.B.P.S. and Madala, S. (2016) Sensitivity of PBL schemes of the WRF-WRF-ARW model in simulating the boundary layer flow parameters for their application to air pollution dispersion modeling over a tropical station. *Atmósfera*, 29, 61–81.

Shin, H.H. and Hong, S.Y. (2011) Intercomparison of planetary boundary-layer parameterizations in the WRF model for a single day from CASES-99. *Boundary Layer Meteorology*, 139, 261–281.

Shrivastava, R., Dash, S.K., Oza, R.B. and Hegde, M.N. (2015) Evaluation of parameterization schemes in the weather research and forecasting (WRF) model: a case study for the Kaiga nuclear power plant site. *Annals of Nuclear Energy*, 75, 693–702.

Singh, J., Yeo, K., Liu, X., Hosseini, R. and Kalagnanam, J.R. (2015) Evaluation of WRF model seasonal forecasts for tropical region of Singapore. *Advances in Science and Research*, 12, 69–72.

Singh, K.S., Subbareddy, B., Purvaja, R., Robin, R.S., Kannan, B.A.M. and Ramesh, R. (2017) Prediction of heavy rainfall over Chennai Metropolitan City, Tamil Nadu, India: impact of microphysical parameterization schemes. *Atmospheric Research*, 202, 219–234.

Sistla, G., Zhou, N., Hao, W., Ku, J.Y., Rao, S.T., Bornstein, R., Freedman, F. and Thunis, P. (1996) Effects of uncertainties in meteorological inputs on urban airshed model predictions and ozone control strategies. *Atmospheric Environment*, 30, 2011–2025.

Skamarock, W.C., Klemp, J.B., Dudhia, J., Gill, D.O., Barker, D.M., Dudha, M. G., Huang, X., Wang, W. and Powers Y. 2008. A Description of the Advanced Research WRF Ver. 30. In: *NCAR Technical Note. NCAR/TN-475STR.* Meso-scale and Micro-scale Meteorology Davison, National Centre for Atmospheric Research, Boulder, Colorado, USA, 113 p.

Tan, E., Mentes, S., Unal, E., Onol, B., Unal, Y.S., Yilmaz, E., Sayinta, M., Goktep, N., and Incecik, S. 2013. Performance evaluation of the WRF model for the short term wind energy prediction system (SWEPS) for Turkey. EWEA Wind Power Forecasting Technology Workshop, Rotterdam, December 4–5, 2013.

Tao, W.K., Simpson, J., Baker, D., Braun, S., Chou, M.D., Ferrier, B., Johnson, D., Khain, A., Lang, S., Lynn, B. and Shie, C.L. (2003) Microphysics, radiation and surface processes in the Goddard cumulus ensemble (GCE) model. *Meteorology and Atmospheric Physics*, 82, 97–137.

Yang, Q., Berg, L.K., Pekour, M., Fast, J.D., Newsom, R.K., Stoelinga, M. and Finley, C. (2013) Evaluation of WRF-predicted near-hub-height winds and ramp events over a Pacific northwest site with complex terrain. *Journal of Applied Meteorology and Climatology*, 52(8), 1753–1763.

## SUPPORTING INFORMATION

Additional supporting information may be found online in the Supporting Information section at the end of the article.

**How to cite this article:** Madala S, Salinas SV, Wang J, Liew SC. Customization of the Advanced Research Weather Research and Forecasting model over the Singapore region: impact of planetary boundary layer schemes, land use, land cover and model horizontal grid resolution. *Meteorol Appl*. 2018;1–11. https://doi.org/10.1002/met.1755